

Astrobiology

Astrobiology Manuscript Central: <http://mc.manuscriptcentral.com/astrobiology>

Evaluation of the Tindouf Basin Region in Southern Morocco as an Analog Site for Soil Geochemistry on Noachian Mars

| | |
|-------------------------------------|--|
| Journal: | <i>Astrobiology</i> |
| Manuscript ID | AST-2016-1557.R3 |
| Manuscript Type: | Research Articles (Papers) |
| Date Submitted by the Author: | 29-Mar-2017 |
| Complete List of Authors: | Oberlin, Elizabeth; Tufts University, Dept. of Chemistry Claire, Mark; University of St. Andrews, Dept. of Earth and Environmental Sciences Kounaves, Samuel; Tufts University, Dept. of Chemistry |
| Keyword: | Mars, Analog, Atacama Desert, Mars Meteorites, Planetary Environments |
| Manuscript Keywords (Search Terms): | Mars analogs, Antarctica, Morocco, oxyanions, nitrate |
| | |

SCHOLARONE™
Manuscripts

1
2
3
4
5
6
7 1
8 2
9
10 3
11 4
12
13 5
14
15
16 6
17 7
18
19 8
20 9
21 10
22 11
23 12
24
25 13
26 14
27 15
28 16
29 17
30 18
31 19
32 20
33 21
34 22
35 23
36 24
37 25
38 26
39 27
40 28
41 29
42 30
43 31
44 32
45 33
46 34
47 35
48 36
49 37
50 38
51 39
52 40
53 41
54 42
55 43
56 44
57 45
58 46
59 47
60 48

Evaluation of the Tindouf Basin Region in Southern Morocco as an Analog Site for Soil Geochemistry on Noachian Mars

Elizabeth A. Oberlin,¹ Mark W. Claire,^{2,3,4} and Samuel P. Kounaves^{1,5}

¹ Department of Chemistry, Tufts University, Medford, Massachusetts

² School of Earth & Environmental Sciences, University of St Andrews, UK

³ Centre for Exoplanet Science, University of St Andrews, UK

⁴ Blue Marble Space Institute of Science, 1001 4th Ave, Seattle, WA USA

⁵ Department of Earth Science & Engineering, Imperial College London, UK

Address correspondence to:

Samuel Kounaves

Department of Chemistry

Tufts University

Medford, MA 02155

E-mail: samuel.kounaves@tufts.edu

Running Title: Tindouf Basin Morocco as a Mars Analog

Submitted to *Astrobiology (Special Issue)***35 Abstract**

36 Locations on Earth which provide insights into processes that may be occurring or
37 may have occurred throughout martian history are often broadly deemed “Mars
38 analog environments.” As no single locale can precisely represent a past or
39 present martian environment, it is important to focus on characterization of
40 terrestrial processes which produce analogous features to those observed in
41 specific regions of Mars, or if possible specific time periods during Martian
42 history. Here, we report on the preservation of ionic species in soil samples
43 collected from the Tindouf region of Morocco and compare them with the
44 McMurdo Dry Valleys of Antarctica, the Atacama Desert in Chile, the Mars
45 meteorite EETA79001, and the in-situ Mars analyses from the Phoenix Wet
46 Chemistry Laboratory (WCL). The Morocco samples show the greatest similarity
47 with those from Victoria Valley (VV), Beacon Valley (BV) and the Atacama,
48 while being consistently depleted compared to University Valley (UV) and
49 enriched compared to Taylor Valley (TV). The NO_3/Cl ratios are most similar to
50 VV and Atacama while the SO_4/Cl ratios are similar to those from BV, VV, and
51 the Atacama. While perchlorate in the Morocco samples are typically lower than
52 other analog sites, conditions in the region are sufficiently arid to retain
53 oxychlorines at detectable levels. Our results suggest that the Tindouf Basin in
54 Morocco can serve as a suitable analog for the soil geochemistry and subsequent
55 aridification of the Noachian epoch on Mars.

57 Kew words or phrases:

58 Mars analogs, Antarctica, Morocco, oxyanions, perchlorate, nitrate

59

60 1. Introduction

61 The obliquity of Mars has fluctuated throughout the historical martian epochs
62 (Ward, 1973; Touma and Wisdom, 1993; Laskar et al., 2004) causing variations
63 in climate that likely resulted in warmer conditions than are presently observed.
64 Phyllosilicate and evaporite minerals at discrete but globally distributed
65 locations on the surface (Langevin *et al.*, 2005; Mangold *et al.*, 2012; Bibring *et*
66 *al.*, 2006; Ehlmann *et al.*, 2013; McLennan *et al.*, 2005; Wray *et al.*, 2009;
67 Arvidson *et al.*, 2014; Toon *et al.*, 1980) support the hypothesis that liquid water
68 influenced the martian surface in the past and that the current state of Mars
69 results from the prolonged aridification of the martian environment as aqueous
70 availability decreased with time. The pedogenic processes that occurred during
71 these episodes distributed soluble ionic species that remain as geochemical
72 proxies that can be used to interpret historical climate patterns.

73 The relative ratios and distribution patterns of salts and their highly soluble
74 anions are commonly examined in order to understand the effects of different
75 degrees of aridity on the geochemical record (Claridge and Campbell, 1977;
76 Cary *et al.*, 1979; Bao *et al.*, 2004; Ewing *et al.*, 2006; Keys and Williams,
77 1981; Zhu and Yang, 2010; Tamppari *et al.*, 2012; Toner *et al.*, 2013; Jackson *et*
78 *al.*, 2015). The distribution profiles of accumulated salts in arid soils is a
79 function of their production rates and the duration of aridity. The primary sink
80 for these salts in temperate climates is rainwater flushing of soils to rivers and

Submitted to *Astrobiology (Special Issue)*

1
2
3
4
5
6
7 81 groundwater, while in polar regions, mobilization by snowmelt or deliquescence
8
9 82 dominates. Thus, comparing environments with similar production mechanisms
10
11 83 (generally atmospheric) but differing degrees of aridity can provide insight into
12
13 84 the geochemical mechanisms that may have acted during the prolonged
14
15 85 aridification of the martian surface. Here, we compare and contrast the ratios of
16
17 86 soluble ions in previously suggested “Mars analog” environments with the
18
19 87 Tindouf Basin, Morocco, specifically the region of the strewn field of the Mars
20
21 88 meteorite, Tissint (Aoudjehane *et al.*, 2012). In particular, we argue that there is
22
23 89 no such thing as a unique terrestrial Mars analog locale – rather that Earth
24
25 90 contains multiple locations which may serve as analogs for various specific
26
27 91 processes at distinct time periods in martian history.
28
29
30
31
32
33
34

35 93 *1.1. Introduction to Terrestrial Environments proposed as “Mars Analogs”*

36
37 94 1.1.1. McMurdo Dry Valleys, Antarctica. Due to their prolonged state as
38
39 95 cold hyperarid deserts, the McMurdo Dry Valleys (MDV) are the most similar of
40
41 96 any terrestrial site to the environmental and geological conditions on Mars (both
42
43 97 past and present) and thus have been widely used as geochemical and geological
44
45 98 martian analogs (Mahaney, 2001; Dickinson and Rosen, 2003; Tamppari *et al.*,
46
47 99 2012; Stroble *et al.*, 2013). While the dry valleys are named as such due to their
48
49 100 complete lack of rainfall, except for a few reported instances in coastal MDV they
50
51 101 experience precipitation in the form of snowfall, often blown in by the winds.
52
53
54
55
56
57
58
59
60

1
2
3
4
5
6
7 102 Most of this snow sublimates in the summer, but there is transfer between
8
9 103 snow/soil/permafrost profiles which influences anion profiles (Toner *et al.*, 2013).
10
11 104 The different valleys within the MDV can be classified within three distinct
12
13 105 climate regions depending on elevation and distance from the coast, which vary in
14
15 106 temperature and aqueous availability (Marchant and Head, 2007). Individual
16
17 107 valleys can thus be compared in order to understand the effects of the changing
18
19 108 martian climate on soil geochemistry. In this way, the relative concentrations of
20
21 109 soluble salts between the lower-elevation Taylor Valley (TV), mid-elevation
22
23 110 Beacon Valley (BV), through the highest-elevation University Valley (UV)
24
25 111 (Tamppari *et al.*, 2012; Stroble *et al.*, 2013; Jackson *et al.*, 2016), can potentially
26
27 112 provide insight into the shift in salt accumulation from the martian Noachian to
28
29 113 the early Amazonian epochs. These localized environments, which can serve as
30
31 114 geochemical analogs throughout the most abrupt climate change periods on Mars,
32
33 115 is a uniquely valuable feature of the MDV. However, their remote location and
34
35 116 extreme environment hinders accessibility.

36
37
38
39
40
41 117 1.1.2. Atacama Desert, Chile. The Atacama Desert is the most arid
42
43 118 nonpolar desert on Earth. Sedimentological data suggests that it has existed as a
44
45 119 stable arid region for the past 150 Ma (Hartley *et al.*, 2005), with evidence of
46
47 120 cyclic variations between arid and hyperarid over the past 14 Ma (Jordan *et al.*,
48
49 121 2014). Although the average temperatures in the Atacama of about 16°C (McKay
50
51 122 *et al.*, 2003) are much warmer than modern Mars, the hyperarid core of the
52
53
54
55
56
57
58
59
60

Submitted to *Astrobiology (Special Issue)*

1
2
3
4
5
6
7 123 Atacama features Earth's lowest total precipitation, measured at < 1 mm/yr in the
8
9 124 Yungay region (Navarro-González *et al.*, 2003), with even more hyperarid
10
11 125 subregions recently identified (Azua-Bustos *et al.*, 2015). The soils found in the
12
13 126 Atacama are characterized by high levels of oxyanions such as sulfate (SO₄²⁻),
14
15 127 nitrate (NO₃⁻), and perchlorate (ClO₄⁻), as the result of atmospheric or volcanic
16
17 128 deposition and input from coastal fog in some regions (Jackson *et al.*, 2005; Bao
18
19 129 *et al.*, 2004; Michalski *et al.*, 2004). The relative accessibility of the Atacama has
20
21 130 yielded key insights into the geochemistry of hyperarid soils and the processes
22
23 131 that drive them (Bao *et al.*, 2004; Ewing *et al.*, 2006; Hartley *et al.*, 2005).

24
25
26
27
28 132 1.1.3. Other warm deserts. In order to interpret data from hyperarid soils
29
30 133 on Earth in terms of historical martian climates, it is necessary to extend these
31
32 134 insights across degrees of aridity. Hyperarid soils on Earth are typically static
33
34 135 under relevant timescales. Therefore, it is necessary to characterize environments
35
36 136 with similar geologic characteristics but different degrees of aridity for
37
38 137 comparison. In this way, we can identify and differentiate the critical processes in
39
40 138 these regions and potentially relate soil geochemistry to various martian epochs.
41
42 139 The Moroccan desert has previously been proposed as Mars-relevant for
43
44 140 operations testing (Ori *et al.*, 2011). Here, we examine the northern Tindouf
45
46 141 basin in southeastern Morocco as a region suitable for use as an analog for soil
47
48 142 chemistry and aqueous geochemistry across different martian epochs.
49
50
51
52

53
54
55
56
57
58
59
60
143

1
2
3
4
5
6
7 144 **2. Materials and Methods**

8
9 145 *2.1. Climate and Geology of Sample Site*

10
11 146 The study region is located on the northern edge of the Tindouf basin, in the
12
13 147 strewn field from which the Tissint Mars meteorite fragments were recovered.

14
15 148 The site is located between the El Aglâb mountains to the north and the Hamada
16
17 149 Du Drâa desert to the south, near the El Ga'ïdat plateau (centered within a ~6km
18
19 150 radius around 29°29'41.29"N, 07°34'50.50"W) (Aoudjehane *et al.*, 2012) (Fig. 1).

20
21 151 Broadly speaking, the environment is an inland desert (~220 km inland) free of
22
23 152 any evaporitic and sabkha features. The basin, located in the foothills on the
24
25 153 southern margin of the Atlas Mountains, feeds into the Draa River (Oued Draa)
26
27 154 watershed, which is dry most of the year at this location, consistent with the
28
29 155 present day climate of a warm arid desert (Peel *et al.*, 2007). The Tindouf basin
30
31 156 contains approximately an 8km thick base layer of Cambrian to Carboniferous
32
33 157 marine sediment with approximately 100 m of Pliocene soils deriving from the
34
35 158 Atlas Mountains above it (Selley, 1997) and atmospheric input (this study). The
36
37 159 study area is near the border with Algeria, and lies entirely within a restricted-
38
39 160 accessed zone controlled by the Moroccan military. The area is uninhabited and
40
41 161 historically only used for military patrols along well-defined 4x4 tracks, although
42
43 162 it has recently experienced substantial foot traffic by Bedouins seeking fragments
44
45 163 of the Tissint meteorite.
46
47
48
49
50
51
52
53
54
55
56
57
58
59
60

Submitted to *Astrobiology (Special Issue)*

1
2
3
4
5
6
7 164 We divided the study site into two geographically distinct, but physically
8
9 165 proximate regions in order to evaluate the influence of the landform variations on
10
11 166 the soluble chemistry of the soils. The Ga'ïdat region is located at the southern
12
13 167 edge of the site at an average elevation of 400 ± 15 m and consists of a plateau
14
15 168 exhibiting little fluvial influence with stable well-developed surface features. The
16
17 169 Aglâb region is located at the northern edge of the study site at the base of a
18
19 170 mountain with an average elevation of 380 ± 0.5 m. The Aglâb region is
20
21 171 characterized by alluvial fans, dry river beds, and variable topography indicative
22
23 172 ephemeral streams and other fluvial processes temporarily feeding the River Draa.

24 25 26 27 28 173 **2.2. Sampling Procedures**

29
30 174 Soil samples were collected from six sites (at 11 pits) in the Aglâb region and
31
32 175 from six sites (at 9 pits) in the Ga'ïdat region (Fig. 1). Sampling sites were
33
34 176 chosen in flat surfaced areas at local topographic highs, without vegetation or foot
35
36 177 tracks, generally with loose to consolidated desert pavement. At each sampling
37
38 178 site two shallow pits were dug to a depth of 20 cm; one at a location in which the
39
40 179 soil was covered with desert pavement, and a second at a similar location nearby
41
42 180 without substantial pavement (Fig. 2). At each site, any surface cobbles were
43
44 181 removed, and a "surface" soil/silt sample from 0-5 cm, and a "depth" sample from
45
46 182 15-20 cm were collected and sealed in pre-sterilized Whirl-Pak® sample bags.
47
48 183 The sampling depth was chosen as a layer of caliche was encountered in most
49
50
51
52
53
54
55
56
57
58
59
60

1
2
3
4
5
6
7 184 areas beginning at 20-30 cm. This was repeated throughout the sampling field to
8
9 185 obtain a well-represented coverage of the area.

10 11 186 *2.3. Soluble Content Analysis*

12
13
14 187 Soil samples were returned to the laboratory and split into sand (2 mm-75
15
16 188 μm) and fine ($< 75 \mu\text{m}$) fractions prior to leaching. A 1.0 g portion of both
17
18 189 fractions of each sample was leached at a 1:10 soil:water ratio for 1 hour with
19
20
21 190 rocking on a Thermoline Labquake and an aliquot of each leachate was then
22
23 191 diluted to a conductivity of 50 $\mu\text{S}/\text{cm}$. The undiluted samples were analyzed for
24
25 192 perchlorate (ClO_4^-) and the diluted samples for inorganic anions by ion
26
27
28 193 chromatography using a Dionex ICS2000 under the conditions listed in Table 1.
29
30 194 Final concentrations for soil samples were determined by accounting for dilutions
31
32 195 and summing the resulting concentrations, weighted by their compositional
33
34
35 196 percentage.

36 37 197 *2.4. Comparative Studies*

38
39
40 198 Ionic concentration of samples from this study were compared to soils in five
41
42 199 other terrestrial sites of differing aridity and temperature, as well as leachate of
43
44 200 the Mars meteorite EETA79001, and the in-situ Mars soil analyses performed by
45
46 201 the Wet Chemistry Laboratory (WCL) on board the Mars Phoenix Lander. The
47
48
49 202 soluble ionic distributions in these regions are compared in terms of the
50
51 203 differences between preservation potential in these locales, with speculative links
52
53
54 204 to soil geochemistry in different Martian epochs.

Submitted to *Astrobiology (Special Issue)*

205

206 **3. Results**

207 The measured anion content of the soil for the Aglâb and Ga'ïdat sampling
208 regions is shown in Table 2. In both regions the particle size distributions
209 generally consist of a primarily sandy soil with a tendency for fine grained
210 particles to accumulate on the surface. The average particle distributions for
211 depth and surface samples are 90-95 wt% and 75-90 wt% sand particles
212 respectively. A neutral soil pH is observed across the entire study region with an
213 average pH of 7.1 ± 0.5 across all samples and differences between surface and
214 subsurface pH values ranging from 0.3-2%. The electrical conductivity (EC) is
215 less consistent across samples with the RSD values ranging from 130-200% both
216 within and across regions, suggesting a heterogeneous distribution of salts,
217 consistent with variability in our ionic measurements. The EC and pH values for
218 each pit at each site are listed in Table 3. The ionic concentrations are generally
219 higher at depth than at the surface (Table 2). This is especially notable for
220 perchlorate which is below the limit of detection (LOD) of 2.5×10^{-4} mmol/kg in
221 surface samples, but present at up to 2.5×10^{-3} mmol/kg (250 ppb) at 20cm.

222 The relative distribution of oxyanions is used to assess the differences
223 between regions by normalizing against total measured anionic content. This
224 allows for the comparison of the relative distribution patterns between samples
225 without the confounding influence of variable salinity due to differential

1
2
3
4
5
6 226 preservation and transport. Fig. 3 shows the interquartile range (IQR) for the
7
8
9 227 distribution of anions, normalized against the total measured anionic content.
10
11 228 Chloride molar fractions exhibit the greatest variability within sampling regions,
12
13 229 and nitrate the smallest. However, nitrate molar fractions exhibit the largest
14
15 230 difference between samples sites, with a 72% difference in medians and a 39%
16
17 231 difference in the IQR between the Aglâb and Ga'ïdat regions. This is compared
18
19 232 to a 48% and 2% difference in median and IQR for chloride and a 2% and 7%
20
21 233 difference in median and IQR for sulfate. Surface and depth molar fractions tend
22
23 234 to be more consistent between the ions with the median difference of 25%, 10%,
24
25 235 and 23% for chloride, sulfate, and nitrate, respectively, while IQR values differed
26
27 236 by 20%, 20%, and 15%, respectively. However, differences in IQR for all ions
28
29 237 and the difference in median for sulfate, are greater between surface and depth
30
31 238 samples, than between sampling regions. Fig. 4 shows the relationship between
32
33 239 the concentrations of oxyanions (sulfate, nitrate, and perchlorate) and the chloride
34
35 240 for the Moroccan soil samples from this study.
36
37
38
39
40
41
42
43
44
45

46 **4. Discussion**

47
48 243 The relatively similar normalized ionic ratios observed throughout the two
49
50 244 sampling regions can be summarized as an overall similarity in terms of salt
51
52 245 origin, resulting in a geochemically homogenous area with outlier sample
53
54
55
56
57
58
59
60

Submitted to *Astrobiology (Special Issue)*

1
2
3
4
5
6 246 variations due to disparate localized transport processes. This is supported by a
7
8
9 247 greater difference in the more soluble nitrate and chloride ions than sulfate, which
10
11 248 would result from the distribution of these highly soluble anions in response to
12
13 249 intermittent precipitation events and diurnal condensation.
14
15

16 250 The difference in the concentrations between the surface and the subsurface
17
18 251 samples is larger than for the samples from the two regions. This is likely the
19
20 252 result of differences in the availability of water to percolate through the soil and
21
22 253 ubiquitous surface mixing by aeolian processes. The higher elevation, better
23
24 254 developed soil profiles on the Ga'ïdat plateau are generally less susceptible to
25
26 255 variation, as evidenced by smaller relative standard deviations in both surface and
27
28 256 depth conductivity measurements, likely due to the limited transport processes
29
30 257 occurring in the region. On the other hand, the more complex Aglâb region, with
31
32 258 its input from aqueous discharge from the nearby mountain and channeling from
33
34 259 the surrounding areas in response to the surrounding higher elevation landforms,
35
36 260 results in greater variation depending on sampling location. Geomorphological
37
38 261 differences aside, the regions can be reasonably considered to be the same in
39
40 262 terms of their normalized soluble anion content and are treated as such for further
41
42 263 comparison purposes.
43
44
45
46
47

48 264 Perchlorate is one the most soluble naturally-occurring salts, so its presence
49
50 265 near the surface implies either an extreme lack of rainfall, or a barrier to vertical
51
52 266 diffusion. At the hyper-arid core of the Atacama Desert, where rainfall averages
53
54
55
56
57
58
59
60

1
2
3
4
5
6 267 less than 1 mm yr⁻¹ (McKay *et al.* 2003), perchlorate is generally leached from
7
8
9 268 soil profiles to at least 50 cm depth (Jackson *et al.* 2015), presumably via
10
11 269 exceedingly rare large rainfall events. In the Tindouf, significant rainfall events
12
13 270 are typical in the winter months, thus we hypothesize the sporadic perchlorate
14
15 271 abundances observed at 15-20 cm depth (from LOD to 2.5×10⁻³ mmol/kg), reflect
16
17 272 a localized hydrological control dominated by a vertical barrier at the hardpan
18
19 273 caliche. In addition to plant uptake (which does not apply to our sample sites),
20
21 274 local geomorphological effects have been shown to cause similar heterogeneity in
22
23 275 the Armargosa desert (Andraski *et al.* 2014). There, measured perchlorate
24
25 276 deposition fluxes of 3.4 ng cm⁻² y⁻¹ agree with higher-end theoretical predictions
26
27 277 of atmospheric perchlorate production from the Atacama desert (Catling *et al.*
28
29 278 2010). Assuming these perchlorate production rates apply to the Tindouf, this
30
31 279 yields an ~ 10³ year accumulation time for the 2.5×10⁻³ mmol/kg observed at 20
32
33 280 cm depth. We speculate that the caliche layer plays a role in the concentration of
34
35 281 soil anions, absorbing moisture from significant rainfall events followed by
36
37 282 extreme evaporation, and that only very significant rainfall years would flush out
38
39 283 the entire system into the Draa River.
40
41
42
43
44
45
46
47
48

285 4.1. Comparison with Other Proposed Mars Analog Sites

286 On Earth, nitrate, chloride, and perchlorate in arid and semi-arid soils are
287 known to be primarily of atmospheric origin (Michalski *et al.*, 2004 ; Bao *et al.*,

Submitted to *Astrobiology (Special Issue)*

1
2
3
4
5
6 288 2004). These ions are also highly water soluble and tend to accumulate in arid
7
8 289 and semi-arid environments (Walvoord *et al.*, 2003 ; Jackson *et al.*, 2015). As a
9
10 290 result, the ratio of these ions in desert soils can be used in the interpretation of the
11
12 291 aqueous processes in these areas. Fig. 5 shows the correlation between the
13
14 292 concentrations of oxyanions and chloride concentrations for sulfate, nitrate, and
15
16 293 perchlorate, for samples from Morocco (linear fit lines from Fig. 4) compared to
17
18 294 samples, from five terrestrial Mars analog sites (Stroble *et al.*, 2013; Tamppari *et*
19
20 295 *al.*, 2012), the Mars meteorite EETA790001 (Kounaves *et al.*, 2014), and the
21
22 296 Mars Phoenix WCL analyses (Kounaves *et al.*, 2010).

23
24
25
26
27 297 4.1.1. Atacama. Samples from the Atacama are similar to Morocco in their
28
29 298 NO_3/Cl ratios and correlation (Fig. 5a), but differ in their NO_3/ClO_4 ratio (Fig. 7)
30
31 299 which is lower than in Morocco. The prolonged hyper-arid conditions in the
32
33 300 Atacama compared to Morocco may explain the lower NO_3/ClO_4 ratio observed in
34
35 301 the Atacama. Since ClO_4^- is highly soluble and is quickly transported in the
36
37 302 presence of water, the prolonged hyper-arid conditions in this region would result
38
39 303 in the greater accumulation of ClO_4^- , reducing the NO_3/ClO_4 ratio.

40
41
42
43
44 304 4.1.2. Beacon Valley. The Beacon Valley samples have comparable NO_3/Cl
45
46 305 and SO_4/Cl ratios to those observed in the Moroccan samples (Fig. 5b). However,
47
48 306 the correlations in both cases demonstrate a greater increase in oxyanion species
49
50 307 compared with Cl^- in Beacon Valley. This consistently larger relative increase
51
52 308 associated with samples from Beacon Valley indicate a preference for
53
54
55
56
57
58
59
60

1
2
3
4
5
6 309 accumulation of oxyanions compared to chloride. This may be due to the higher
7
8
9 310 elevation of Beacon Valley which results in less input of Cl^- from ocean spray
10
11 311 and/or a more rapid accumulation of atmospherically derived oxyanion species.
12
13 312 Both NO_3^- and ClO_4^- are highly soluble, and their persistence in an environment is
14
15 313 indicative of the relative absence of aqueous transport processes. The correlation
16
17 314 between NO_3^- , ClO_4^- , and Cl for Beacon Valley falls in the center when compared
18
19 315 with the other investigated analog environments (Figs 6 and 7) suggesting that
20
21 316 Beacon Valley is an intermediate in terms of the processes driving ionic ratios in
22
23 317 these areas.

24
25
26
27
28 318 4.1.3. University Valley. The University Valley $\text{NO}_3^-/\text{ClO}_4^-$ ratios are the
29
30 319 most similar to the Morocco samples (Fig. 7), but no other similarities are
31
32 320 observed between the data sets. In general, oxyanion ratios and correlations are
33
34 321 much larger and steeper in University Valley than other analog sites (Fig. 5c).
35
36 322 This is similar to the observations for Beacon Valley, wherein oxyanions
37
38 323 accumulate and Cl^- input is minimal, but extended to a more arid environment.

39
40
41 324 4.1.4. Taylor Valley. For Taylor Valley the NO_3^- is well correlated with Cl^-
42
43 325 ($R^2 = 0.90$) with a comparable slope to that observed in the Moroccan samples,
44
45 326 but is relatively depleted in NO_3^- with respect to Cl^- (Fig. 5d). NO_3^- is similarly
46
47 327 well correlated to ClO_4^- ($R^2 = 0.85$) with the shallowest slope observed across all
48
49 328 investigated analog sites (Fig. 6), and a two order of magnitude shallower slope
50
51 329 than is observed in Morocco. In general, Oxyanion/ Cl ratios are lower and
52
53
54
55
56
57
58
59
60

Submitted to *Astrobiology (Special Issue)*

1
2
3
4
5
6
7 330 oxyanions tend to accumulate less compared to Cl^- in Taylor Valley than in
8
9 331 Morocco, with the exception of an enrichment of ClO_4^- relative to Cl^- . This may
10
11 332 be the result of an increase in Cl^- compared with NO_3^- in Taylor Valley, as a result
12
13 333 of input from ocean water spray.

14
15
16 334 4.1.5. Victoria Valley. The Victoria Valley samples are the most similar of
17
18 335 the investigated sites to the Moroccan samples (Fig. 5e). Specifically, comparable
19
20 336 ratios are observed between the regions for $\text{NO}_3^-/\text{Cl}^-$ and $\text{NO}_3^-/\text{ClO}_4^-$ (Fig. 7).
21
22
23 337 However, while $\text{NO}_3^-/\text{ClO}_4^-$ ratios exhibit a similar correlation between the regions,
24
25 338 Victoria Valley has an order of magnitude steeper slope in $\text{NO}_3^-/\text{Cl}^-$ correlation
26
27 339 compared with Morocco. The similarity in ratios, but difference in linear fit for
28
29 340 Victoria Valley samples is likely related to differences in post-depositional
30
31 341 processes such as aqueous transport, which may be more complicated in Victoria
32
33 342 Valley compared with Morocco in part due to influences from shallow
34
35 343 groundwater and permafrost in this polar region (Levy *et al.*, 2011; Marchant and
36
37 344 Head, 2007).

345 4.2. Comparison to Direct Measurements on Mars Samples

346 Figure 5f shows our results in comparison with two direct measurements of
347 soluble species in martian samples, one from the in-situ WCL analyses of martian
348 soil by the Phoenix Mars Lander (Kounaves *et al.*, 2010) and the other from a
349 carbonate clast in the Mars meteorite EETA79001 (Kounaves *et al.*, 2014). In
350 general, oxyanion species are more concentrated in both the WCL and
351
352
353
354
355
356
357
358
359
360

1
2
3
4
5
6
7 351 EETA79001 samples, while Cl^- is depleted. Of note is the similarity between the
8
9 352 relative SO_4^{2-} , NO_3^- , and ClO_4^- values in EETA79001 measurements compared to
10
11 353 the Moroccan samples. In general, it is observed that SO_4/Cl , NO_3/Cl and
12
13 354 ClO_4/Cl ratios are consistently and similarly higher in EETA79001. Also, of note
14
15 355 is the large concentration of ClO_4^- that was measured by the Phoenix WCL
16
17 356 compared to EETA79001. This may be indicative of a steady increase in ClO_4^-
18
19 357 concentration over time as Cl^- has been shown to be easily oxidized to ClO_4^- on
20
21 358 mineral surfaces (Carrier and Kounaves, 2015). A similar tendency is noted in
22
23 359 the analog sites wherein ClO_4/Cl ratios increase with increasing aridity. This
24
25 360 observation supports the proposition that the higher aridity locales such as
26
27 361 University Valley can serve as analogs to more recent martian epochs while the
28
29 362 less arid Victoria Valley would serve as an analog to earlier epochs.

35 363 *4.3. Comparison to The Martian Epochs*

36
37 364 A summary of the martian epochs and their proposed corresponding
38
39 365 terrestrial analogs are shown in Fig. 8. If we consider the MDV as analogs to the
40
41 366 different martian epochs depending on the extent of aqueous influence, we find
42
43 367 that it decreases in the order University Valley > Beacon Valley > Victoria Valley
44
45 368 > Taylor Valley. In this way, University and Beacon Valley can be roughly
46
47 369 considered as analogs to the Amazonian/Hesperian epochs, and Taylor and
48
49 370 Victoria Valleys to the Hesperian/Noachian epochs. Due to the greater
50
51 371 similarities between the lower elevation Victoria Valley and the Moroccan
52
53
54
55
56
57
58
59
60

Submitted to *Astrobiology (Special Issue)*

1
2
3
4
5
6
7 372 samples as compared to the higher elevation University Valley samples, and the
8
9 373 likelihood that these similarities are the result of the greater influence of aqueous
10
11 374 processes in these regions, we argue that the Moroccan sample locations are
12
13 375 potential soil geochemistry analogs to the late Noachian epoch on Mars.
14
15

16 376 **5. Conclusions**

17
18
19 377 The utility of the Tindouf Basin region of southeastern Morocco as a more
20
21 378 accessible analog with a similar soil geochemistry to the MDVs is demonstrated
22
23 379 by the relative similarity of the distribution of ionic species between the
24
25 380 Moroccan samples and other Mars analog sites. In general, samples from this
26
27 381 region of Morocco show the greatest similarity with samples from Victoria
28
29 382 Valley, Beacon Valley and the Atacama. Moroccan samples are consistently
30
31 383 depleted in oxyanion species compared to University Valley and enriched
32
33 384 compared with Taylor Valley. Specifically, NO_3/Cl ratios are comparable to
34
35 385 many proposed Mars analog sites, with the strongest similarities observed with
36
37 386 Victoria Valley and Atacama samples. The SO_4/Cl ratios are likewise similar to
38
39 387 those from Beacon Valley, Victoria Valley, and in the Atacama. While
40
41 388 perchlorate values in Morocco are typically lower than other analog sites,
42
43 389 conditions in the region are sufficiently arid to retain oxychlorines at detectable
44
45 390 levels. Processes that may have preferentially increased the perchlorate in other
46
47 391 regions could include rapid aqueous accumulation and evaporation of the highly
48
49 392 soluble oxychlorines, or the production by direct UV oxidation of chlorine in
50
51
52
53
54
55
56
57
58
59
60

1
2
3
4
5
6 393 chloride-bearing minerals, as has been suggested to occur on Mars (Carrier and
7
8
9 394 Kounaves, 2015). The perchlorate in the Morocco samples is most likely a result
10
11 395 of slow accumulation via atmospheric production as occurs over most of the Earth
12
13 396 (Catling *et al.*, 2010) though direct UV oxidation cannot be entirely ruled out.
14
15

16 17 397 **Acknowledgements**

18
19 398 We would like to thank Joseph Levy and the anonymous reviewers who helped
20
21 399 improve this manuscript. We also thank the Ibn Battuta Centre in particular Gian
22
23 400 Gabriele Ori and Kamal Taj-Edine for their assistance with logistics and fieldwork.
24
25
26 401 In addition, we would like to thank the Moroccan military for access as well as
27
28 402 Aubrey Zerkle and Gordon Fontaine for their assistance in the field.
29
30

31 403 **Disclosure Statement**

32
33 404 No competing financial interests exist.
34
35
36

37 405

38 39 406 **References**

40
41 407 Andraski, B. J., W. A. Jackson, T. L. Welborn, J. K. Böhlke, R. Sevanthi, and
42
43 408 D.A. Stonestrom. (2014) Soil, Plant, and Terrain Effects on Natural
44
45 409 Perchlorate Distribution in a Desert Landscape. *J. Environ. Qual.* 43:980-994
46
47
48
49 410
50
51 411 Aoudjehane, H.C., Avice, G., Barrat, J-A., Boudouma, O., Chen, G., Duke, M.J.
52
53 412 M., Franchi, I.A., Gattacceca. J., Grady, M.M., Greenwood, R.C., Herd,
54
55
56
57
58
59
60

Submitted to *Astrobiology (Special Issue)*

- 1
2
3
4
5
6 413 C.D.K., Hewins, R., Jambon, A., Marty, B., Rochette, P., Smith, C.L.,
7
8 414 Sautter, V., Verchovsky, A., Weber, P., and Zanda, B. (2012) Tissint
9
10 415 Martian Meteorite: A Fresh Look at the Interior, Surface, and Atmosphere of
11
12 416 Mars. *Science* 338:785-788.
13
14
15
16 417 Arvidson, R.E., Squyres, S.W., Bell, J.F., Catalano, J.G., Clark, B.C., Crumpler,
17
18 418 L.S., de Souza, P.A., Fairén, A.G., Farrand, W.H., Fox, V.K., Gellert, R.,
19
20 419 Ghosh, A., Golombek, M.P., Grotzinger, J.P., Guinness, E.A., Herkenhoff,
21
22 420 K.E., Jolliff, B.L., Knoll, A.H., Li, R., McLennan, S.M., Ming, D.W.,
23
24 421 Mittlefehldt, D.W., Moore, J.M., Morris, R.V., Murchie, S.L., Parker, T.J.,
25
26 422 Paulsen, G, Rice, J.W., Ruff, S.W., Smith, M.D., and Wolff, M. J. (2014)
27
28 423 Ancient Aqueous Environments at Endeavour Crater, Mars. *Science* 343
29
30 424 (6169): 1248097.
31
32
33
34
35 425 Azua-Bustos, A., Caro-Lara, L., and Vicuna, R. (2015) Discovery and Microbial
36
37 426 Content of the Driest Site of the Hyperarid Atacama Desert, Chile. *Environ.*
38
39 427 *Microbio.Rep.* 7:388-394.
40
41
42
43 428 Bao H., Jenkins K.A., Khachatryan M., and Díaz G.C. (2004) Different sulfate
44
45 429 sources and their post-depositional migration in Atacama soils. *Earth*
46
47 430 *Planet. Sci. Lett.* 224:577-587.
48
49
50
51 431 Bao H., and Gu B. (2004) Natural Perchlorate Has a Unique Oxygen Isotope
52
53 432 Signature. *Environ. Sci. Technol.*, 38:5073-5077.
54
55
56
57
58
59
60

- 1
2
3
4
5
6 433 Bibring J.P., Langevin Y., Mustard J.F., Poulet F., Arvidson R., Gendrin A.,
7
8 434 Gondet B., Mangold N., Pinet P., Forget F., Berthe M., Bibring J.P., Gendrin
9
10 435 A., Gomez C., Gondet B., Jouglet D., Poulet F., Soufflot A., Vincendon M.,
11
12 436 Combes M., Drossart P., Encrenaz T., Fouchet T., Merchiorri R., Belluci G.,
13
14 437 Altieri F., Formisano V., Capaccioni F., Cerroni P., Coradini A., Fonti S.,
15
16 438 Korablev O., Kottsov V., Ignatiev N., Moroz V., Titov D., Zasova L.,
17
18 439 Loiseau D., Mangold N., Pinet P., Doute S., Schmitt B., Sotin C., Hauber E.,
19
20 440 Hoffmann H., Jaumann R., Keller U., Arvidson R., Mustard J.F., Duxbury
21
22 441 T., Forget F., and Neukum G. (2006) Global mineralogical and aqueous mars
23
24 442 history derived from OMEGA/Mars Express data. *Science*, 312:400-4.
25
26
27
28
29
30 443 Carrier B.L., and Kounaves S.P. (2015) The origins of perchlorate in the Martian
31
32 444 soil. *Geophys. Res. Lett.* 42:3739-3745.
33
34
35
36 445 Cary, J.W., Papendick, R.I., and Campbell, G.S. (1979) Water and Salt Movement
37
38 446 in Unsaturated Frozen Soil: Principles and Field Observations. *Soil Sci. Soc.*
39
40 447 *Am. J.* 43:3-8.
41
42
43 448 Catling D.C., Claire M.W., Zahnle K.J., Quinn R.C., Clark B.C., Hecht M.H., and
44
45 449 Kounaves S. (2010) Atmospheric origins of perchlorate on Mars and in the
46
47 450 Atacama. *J. Geophys. Res.* 115:E00E11.
48
49
50
51 451 Claridge, G.G.C., and Campbell, I.B. (1977) The salts in Antarctic soils, their
52
53 452 distribution and relationship to soil processes. *Soil Science*, 123:377-384.
54
55
56
57
58
59
60

Submitted to *Astrobiology (Special Issue)*

- 1
2
3
4
5
6 453 Dickinson, W.W., and Rosen, M.R. (2003) Antarctic Permafrost: An Analogue
7
8 454 for Water and Diagenetic Minerals on Mars. *Geology* 31:199-202.
9
10
11 455 Ehlmann, B.L., Berger, G., Mangold, N., Michalski, J.R., Catling, D.C., Ruff,
12
13 456 S.W., Chassefière, E., Niles, P.B., Chevrier, V., and Poulet, F. (2013)
14
15 457 Geochemical Consequences of Widespread Clay Mineral Formation in Mars'
16
17 458 Ancient Crust. *Space Sci. Rev.* 174:329-364.
18
19
20
21 459 Ewing, S.A., Sutter, B., Owen, J., Nishiizumi, K., Sharp, W., Cliff, S.S., Perry,
22
23 460 K., Dietrich, W., McKay, C.P., and Amundson, R. (2006) A threshold in soil
24
25 461 formation at Earth's arid-hyperarid transition. *Geochim. Cosmochim. Acta*,
26
27 462 70:5293-5322.
28
29
30
31 463 Hartley, A.J., Chong, G., Houston, J., and Mather, A.E. (2005) 150 Million Years
32
33 464 of Climatic Stability: Evidence from the Atacama Desert, Northern Chile. *J.*
34
35 465 *Geol. Soc.* 162:421-424.
36
37
38
39 466 Jackson, W.A., Davila, A.F., Böhlke, J.K., Sturchio, N.C., Sevanthi, R., Estrada,
40
41 467 N., Brundrett, M., Lacelle, D., McKay, C.P., Poghosyan, A., Pollard, W., and
42
43 468 Zacny, K. (2016) Deposition, accumulation, and alteration of Cl^- , NO_3^- ,
44
45 469 ClO_4^- and ClO_3^- salts in a hyper-arid polar environment: Mass balance and
46
47 470 isotopic constraints. *Geochim. Cosmochim. Acta* 182:197-215.
48
49
50
51 471 Jackson, W.A., Böhlke, J. K., Andraski, B. J., Fahlquist, L., Bexfield, L., Eckardt,
52
53 472 F.D., Gates, J.B., Davila, A.F., McKay, C.P., Rao, B., Sevanthi, R.,
54
55
56
57
58
59
60

- 1
2
3
4
5
6 473 Rajagopalan, S., Estrada, N., Sturchio, N., Hatzinger, P.B., Anderson, T.A.,
7
8 474 Orris, G., Betancourt, J., Stonestrom, D., Latorre, C., Li, Y., and Harvey,
9
10 475 G.J. (2015) Global patterns and environmental controls of perchlorate and
11
12 476 nitrate co-occurrence in arid and semi-arid environments. *Geochim.*
13
14
15 477 *Cosmochim. Acta* 164:502-522.
16
17
18 478 Jackson, W.A., Anderson, T.A., Tian, K., and Tock, R.W. (2005) The Origin of
19
20 479 Naturally Occurring Perchlorate : The Role of Atmospheric Processes.
21
22 480 *Environ. Sci.* 39:1569-1575.
23
24
25 481 Jordan, T.E., Kirk-Lawlor, N.E., Blanco, P.N., Rech, J.A., and Cosentino, N.J.
26
27 482 (2014) Landscape Modification in Response to Repeated Onset of Hyperarid
28
29 483 Paleoclimate States since 14 Ma, Atacama Desert, Chile. *Bull. Geol. Soc.*
30
31 484 *Am.* 126:1016-1046.
32
33
34 485 Keys J.R., and Williams K. (1981) Origin of crystalline, cold desert salts in the
35
36 486 McMurdo region, Antarctica. *Geochim. Cosmochim. Acta* 45:2299-2309.
37
38
39 487 Kounaves, S.P., Hecht, M.H., Kapit, J., Gospodnova, K., DeFlores, L., Quinn,
40
41 488 R.C., Boynton, W.V., Clark, B.C., Catling, D.C., Hredzak, P., Ming, D.W.,
42
43 489 Moore, Q., Shusterman, J., Stroble, S., West, S.J., and Young, S.M.M.
44
45 490 (2010) Wet Chemistry experiments on the 2007 Phoenix Mars Scout Lander
46
47 491 mission: Data analysis and results. *J. Geophys. Res.*, 115:E00E10.
48
49
50 492 Kounaves, S.P., Carrier, B.L., O'Neil, G.D., Stroble, S.T., and Claire, M.W.
51
52
53
54
55
56
57
58
59
60

Submitted to *Astrobiology (Special Issue)*

- 1
2
3
4
5
6 493 (2014) Evidence of martian perchlorate, chlorate, and nitrate in Mars
7
8
9 494 meteorite EETA79001: Implications for oxidants and organics. *Icarus*,
10
11 495 229:206-213.
12
13
14 496 Langevin. Y., Poulet. F., Bibring. J.-P., and Gondet. B. (2005) Sulfates in the
15
16 497 North Polar Region of Mars Detected by OMEGA/Mars Express. *Science*,
17
18 498 307:1584-1586.
19
20
21 499 Laskar, J., A. C. M. Correia, M. Gastineau, F. Joutel, B. Levrard, and P. Robutel
22
23 500 (2004), Long term evolution and chaotic diffusion of the insolation quantities
24
25 501 of Mars, *Icarus*, 170:343-364.
26
27
28
29 502 Levy J.S., Fountain A.G., Gooseff M.N., Welch K.A., and Lyons W.B. (2011)
30
31 503 Water tracks and permafrost in Taylor Valley, Antarctica: Extensive and
32
33 504 shallow groundwater connectivity in a cold desert ecosystem. *Geological*
34
35 505 *Society of America Bulletin*, 123:2295-2311.
36
37
38
39 506 Mahaney, W. (2001) Morphogenesis of Antarctic Paleosols: Martian Analogue.
40
41 507 *Icarus*, 154:113-130.
42
43
44 508 Mangold, N., Carter, J., Poulet, F., Dehouck, E., Ansan, V., and Loizeau, D.
45
46 509 (2012) Late Hesperian Aqueous Alteration at Majuro Crater, Mars. *Planet.*
47
48 510 *Space Sci.* 72:18-30.
49
50
51
52 511 Marchant, D.R., and Head, J.W. (2007) Antarctic dry valleys: Microclimate
53
54 512 zonation, variable geomorphic processes, and implications for assessing
55
56
57
58
59
60

- 1
2
3
4
5
6 513 climate change on Mars. *Icarus*, 192:187-222.
7
8
9 514 McKay C.P., Friedmann E.I., Gómez-Silva B., Cáceres-Villanueva L., Andersen
10
11 515 D.T., and Landheim R. (2003) Temperature and Moisture Conditions for
12
13 516 Life in the Extreme Arid Region of the Atacama Desert: Four Years of
14
15 517 Observations Including the El Niño of 1997–1998. *Astrobiology*, 3:393-406.
16
17
18
19 518 McLennan, S.M., Bell, S.F., Calvin, W.M., Christensen, P.R., Clark, B.C., de
20
21 519 Souza, P.A., Farmer, J., Farrand, W.H., Fike, D.A., Gellert, R., Ghosh, A.,
22
23 520 Glotch, T.D., Grotzinger, J.P., Hahn, B., Herkenhoff, K.E., Hurowitz, J.A.,
24
25 521 Johnson, J.R., Johnson, S.S., Jolliff, B., Klingelhofer, G., Knoll, A.H.,
26
27 522 Learner, Z., Malin, M.C., McSween, Jr H.Y., Pockock, J., Ruff, S.W.,
28
29 523 Soderblom, L.A., Squyres, S.W., Tosca, N.J., Watters, W.A., Wyatt, M., and
30
31 524 Yen, A. (2005) Provenance and Diagenesis of the Evaporite-Bearing Burns
32
33 525 Formation, Meridiani Planum, Mars. *Earth Planet. Sci. Lett.* 240:95-121.
34
35
36
37
38 526 Michalski, G., Böhlke, J.K., and Thiemens, M. (2004) Long term atmospheric
39
40 527 deposition as the source of nitrate and other salts in the Atacama Desert,
41
42 528 Chile: New evidence from mass-independent oxygen isotopic compositions.
43
44 529 *Geochim. Cosmochim. Acta*, 68:4023-4038.
45
46
47
48 530 Navarro-González, R., Rainey, F.A., Molina, P., Bagaley, D.R., Hollen, B.J., de la
49
50 531 Rosa, J., Small, A.M., Quinn, R.C., Grunthaner, F.J., Cáceres, L., Gomez-
51
52 532 Silva, B., and McKay, C.P. (2003) Mars-Like Soils in the Atacama Desert,
53
54
55
56
57
58
59
60

Submitted to *Astrobiology (Special Issue)*

- 1
2
3
4
5
6 533 Chile, and the Dry Limit of Microbial Life. *Science*, 302:1018-1021.
7
8
9 534 Ori, G.G., Taj-Eddine, K., and Dell'Arciprete, I. (2011) The Ibn Battuta Centre
10
11 535 (Marrakech, Morocco) for Testing Lander Science, Operations and Landing
12
13 536 Systems, in *Analogue Sites for Mars Missions: MSL and Beyond*, LPI
14
15 537 Contribution No. 161, Abstract 6006.
16
17
18
19 538 Peel, M.C., Finlayson, B.L., and McMahon, T.A. (2007) Updated World Map of
20
21 539 Köppen-Geiger Climate Classification. *Hydrol. Earth Sys. Sci.* 11:1633-44.
22
23
24 540 Selley, R.C. (1997) Chapter 1 The Sedimentary Basins of Northwest Africa, In
25
26 541 *Sedimentary Basins of the World Vol. 3: African Basins*, 3-16.
27
28
29
30 542 Stroble, S.T., McElhoney, K.M., and Kounaves, S.P. (2013) Comparison of the
31
32 543 Phoenix Mars Lander WCL soil analyses with Antarctic Dry Valley soils,
33
34 544 Mars meteorite EETA79001 sawdust, and a Mars simulant. *Icarus*, 225:933-
35
36 545 939.
37
38
39
40 546 Tamppari, L.K., Anderson, R.M., Archer, P.D., Douglas, S., Kounaves, S.P.,
41
42 547 McKay, C.P., Ming, D.W., Moore, Q., Quinn, J.E., Smith, P.H., Stroble, S.,
43
44 548 and Zent, A.P. (2012) Effects of extreme cold and aridity on soils and
45
46 549 habitability: McMurdo Dry Valleys as an analogue for the Mars Phoenix
47
48 550 landing site. *Antarctic Science*, 24:211-228.
49
50
51
52 551 Toner, J.D., Sletten, R.S., and Prentice, M.L. (2013) Soluble salt accumulations in
53
54 552 Taylor Valley, Antarctica: Implications for paleolakes and Ross Sea Ice
55
56
57
58
59
60

- 1
2
3
4
5
6 553 Sheet dynamics. *J. Geophys. Res. Earth Sur.* 118:198-215.
7
8
9 554 Toon, O.B., Pollack, J.B., Ward, W., Burns, J.A., and Bilski, K. (1980) The
10
11 555 Astronomical Theory of Climatic Change on Mars. *Icarus* 44:552-607.
12
13
14 556 Touma, J, and Wisdom, J. (1993) The Chaotic Obliquity of Mars. *Science*
15
16 557 259:1294-1297.
17
18
19 558 Walvoord M.A., Phillips F.M., Stonestrom D.A., Evans R.D., Hartsough P.C.,
20
21 559 Newman B.D., and Striegl R.G. (2003) A Reservoir of Nitrate Beneath
22
23 560 Desert Soils. *Science*, 302:1021-1024.
24
25
26
27 561 Ward, W. (1973) Large-Scale Variations in the Obliquity of Mars. *Science*
28
29 562 181:260-262.
30
31
32 563 Wray, J.J., Noe Dobrea, E.Z., Arvidson, R.E., Wiseman, S.M., Squyres, S.W.,
33
34 564 McEwen, A.S., Mustard, J.F., and Murchie, S.L. (2009) Phyllosilicates and
35
36 565 sulfates at Endeavour Crater, Meridiani Planum, Mars. *Geophys. Res. Lett.*,
37
38 566 36:L21201.
39
40
41
42 567 Zhu B., and Yang X. (2010) The origin and distribution of soluble salts in the
43
44 568 sand seas of northern China. *Geomorphology*, 123:232-242.
45
46
47
48 569
49
50
51
52
53
54
55
56
57
58
59
60

Submitted to *Astrobiology (Special Issue)*

1
2
3
4
5
6
7
8 570 Table 1: Parameters and reagents used for IC analysis of samples. Columns used
9 571 for all samples were 250mm x 4mm
10

| | Anions | Perchlorate |
|--|---------------|--------------------|
| Dionex Column | AS16 | AS18 |
| Eluent | KOH | KOH |
| Eluent Conc., mM | 20 | 35 |
| Flow Rate, mL/min | 1 | 1.25 |
| Suppressor Current, μS | 75 | 175 |
| Injection Volume, μL | 25 | 100 |

11
12
13
14
15
16
17
18
19
20
21 572
22 573
23
24
25
26
27
28
29
30
31
32
33
34
35
36
37
38
39
40
41
42
43
44
45
46
47
48
49
50
51
52
53
54
55
56
57
58
59
60

574 Table 2: Measured anion concentration data for the Aglâb and Ga'ïdat region
 575 samples

| Surface (0-5 cm) Ion Concentration (mmol/kg) | | | | | | |
|--|--------|------------------|-----------------|----------------|-----------------|---------------------|
| Region | Sample | Chloride | Sulfate | Nitrate | Chlorate | Perchlorate |
| Aglâb | 1a | 3.42 ± 0.123 | 2.85 ± 0.050 | 0.57 ± 0.050 | 0.09 ± 0.010 | ND |
| | 1b | 5.63 ± 0.052 | 15.43 ± 0.111 | 1.06 ± 0.084 | 0.090 ± 0.008 | ND |
| | 2a | 2.34 ± 0.045 | 1.55 ± 0.013 | 0.38 ± 0.015 | 0.06 ± 0.004 | ND |
| | 2b | 2.55 ± 0.008 | 0.20 ± 0.006 | 0.26 ± 0.005 | 0.03 ± 0.002 | ND |
| | 3a | 0.87 ± 0.023 | 1.00 ± 0.007 | 0.45 ± 0.009 | 0.04 ± 0.002 | ND |
| | 3b | 0.45 ± 0.005 | 0.23 ± 0.002 | 0.34 ± 0.002 | 0.02 ± 0.001 | ND |
| | 4a | 44.52 ± 0.395 | 2.34 ± 0.085 | 4.69 ± 0.112 | 0.20 ± 0.025 | ND |
| | 4b | 282.47 ± 1.687 | 36.59 ± 0.331 | 1.45 ± 0.203 | ND | ND |
| | 5a | 26.51 ± 0.073 | 11.13 ± 0.049 | 0.87 ± 0.021 | 0.11 ± 0.009 | ND |
| | 5b | 23.97 ± 0.096 | 11.13 ± 0.024 | 1.54 ± 0.042 | 0.12 ± 0.011 | ND |
| Ga'ïdat | 6a | 1.68 ± 0.148 | 1.94 ± 0.145 | 0.37 ± 0.027 | ND | ND |
| | 7a | 3.86 ± 0.051 | 0.72 ± 0.012 | 0.64 ± 0.015 | 0.06 ± 0.004 | ND |
| | 7b | 3.58 ± 0.019 | 0.14 ± 0.002 | 0.46 ± 0.003 | ND | ND |
| | 8a | 0.31 ± 0.019 | 0.32 ± 0.005 | 0.16 ± 0.007 | 0.03 ± 0.001 | ND |
| | 9a | 0.29 ± 0.019 | 0.22 ± 0.006 | 0.15 ± 0.008 | 0.04 ± 0.003 | ND |
| | 10a | 0.45 ± 0.020 | 0.28 ± 0.007 | 0.27 ± 0.007 | 0.03 ± 0.002 | ND |
| | 11a | 0.34 ± 0.020 | 0.30 ± 0.008 | 0.28 ± 0.007 | 0.05 ± 0.002 | ND |
| | 11b | 0.14 ± 0.003 | 0.13 ± 0.002 | 0.10 ± 0.002 | 0.03 ± 0.001 | ND |
| | 12a | 20.76 ± 0.170 | 1.97 ± 0.045 | 0.76 ± 0.043 | 0.09 ± 0.013 | ND |
| | 12b | 25.31 ± 0.099 | 1.96 ± 0.017 | 0.88 ± 0.023 | 0.10 ± 0.010 | ND |
| Depth (15-20 cm) Ion Concentration (mmol/kg) | | | | | | |
| Region | Sample | Chloride | Sulfate | Nitrate | Chlorate | Perchlorate |
| Aglâb | 1a | 102.89 ± 8.882 | 4.10 ± 1.316 | 11.96 ± 1.071 | ND | 4.7E-04 ± 4.80E-05 |
| | 1b | 14.86 ± 0.128 | 1.31 ± 0.007 | 1.17 ± 0.019 | 0.06 ± 0.006 | 2.56E-04 ± 4.60E-05 |
| | 2a | 131.89 ± 2.542 | 60.01 ± 1.256 | 11.70 ± 0.389 | ND | 5.04E-04 ± 4.69E-05 |
| | 2b | 87.41 ± 1.781 | 11.97 ± 0.199 | 13.23 ± 0.175 | ND | 5.20E-04 ± 4.55E-05 |
| | 3a | 2.67 ± 0.087 | 3.79 ± 0.104 | 1.26 ± 0.032 | 0.06 ± 0.008 | ND |
| | 3b | 0.18 ± 0.004 | 0.11 ± 0.002 | 0.11 ± 0.003 | 0.02 ± 0.001 | ND |
| | 4a | 89.09 ± 62.724 | 31.00 ± 2.776 | 27.87 ± 15.474 | ND | 1.28E-03 ± 4.56E-05 |
| | 4b | 1460.84 ± 15.221 | 231.30 ± 1.165 | 6.33 ± 0.818 | ND | ND |
| | 5a | 151.76 ± 4.374 | 55.72 ± 1.091 | 8.80 ± 0.442 | ND | 4.38E-04 ± 1.23E-04 |
| | 5b | 55.86 ± 1.682 | 37.58 ± 1.562 | 3.26 ± 0.157 | ND | ND |
| Ga'ïdat | 6a | 1.49 ± 0.081 | 6.70 ± 0.032 | 0.13 ± 0.025 | ND | ND |
| | 7a | 15.03 ± 0.384 | 1.27 ± 0.106 | 4.57 ± 0.260 | ND | 2.50E-03 ± 2.02E-05 |
| | 7b | 165.20 ± 1.366 | 24.68 ± 0.071 | 24.65 ± 0.094 | ND | 4.25E-04 ± 2.12E-05 |
| | 8a | 3.17 ± 0.081 | 3.34 ± 0.039 | 1.60 ± 0.034 | 0.07 ± 0.011 | ND |
| | 9a | 21.75 ± 0.583 | 63.88 ± 0.440 | 7.79 ± 0.241 | ND | ND |
| | 10a | 11.08 ± 0.206 | 14.73 ± 0.316 | 6.14 ± 0.123 | ND | 2.72E-04 ± 2.02E-05 |
| | 11a | 2.71 ± 0.064 | 3.66 ± 0.042 | 1.49 ± 0.026 | 0.01 ± 4.83E-04 | ND |
| | 11b | 0.92 ± 0.006 | 1.03 ± 0.005 | 0.57 ± 0.003 | 0.03 ± 0.001 | ND |
| | 12a | 980.52 ± 40.339 | 163.47 ± 10.130 | 121.07 ± 7.713 | 0.56 ± 0.148 | 1.57E-03 ± 3.35E-05 |
| | 12b | 242.80 ± 12.422 | 12.85 ± 0.628 | 21.82 ± 1.211 | ND | 9.01E-04 ± 4.94E-05 |

576

Submitted to *Astrobiology (Special Issue)*

577

578 Table 3: pH, conductivity, and grain size distribution data for the Aglâb and

579 Ga'ïdat region samples

580

| Region | Sample | pH | | EC ($\mu\text{S}/\text{cm}$) | | 2000-75 μm (wt %) | | < 75 μm (wt %) | |
|-----------------|---------|-----------------|-----------------|--------------------------------|---------------------|------------------------------|------------------|---------------------------|------------------|
| | | 0-5 cm | 15-20 cm | 0-5 cm | 15-20 cm | 0-5 cm | 15-20 cm | 0-5 cm | 15-20 cm |
| Aglâb samples | 1a | 6.96 | 6.87 | 146.51 | 1373.16 | 82.7% | 95.0% | 17.3% | 5.0% |
| | 1b | 7.64 | 7.68 | 480.07 | 243.56 | 87.4% | 90.0% | 12.6% | 10.0% |
| | 2a | 7.56 | 6.92 | 123.40 | 2487.04 | 74.8% | 96.0% | 25.2% | 4.0% |
| | 2b | 7.87 | 7.08 | 119.42 | 1374.29 | 86.9% | 90.7% | 13.1% | 9.3% |
| | 3a | 6.86 | 6.81 | 105.14 | 209.37 | 79.9% | 91.2% | 20.1% | 8.8% |
| | 3b | 7.13 | 7.24 | 57.23 | 45.56 | 93.0% | 94.0% | 7.0% | 6.0% |
| | 4a | 7.34 | 6.63 | 594.49 | 7702.38 | 87.9% | 92.0% | 12.1% | 8.0% |
| | 4b | 8.04 | 7.12 | 4033.56 | 17484.78 | 92.2% | 92.3% | 7.8% | 7.7% |
| | 5a | 7.01 | 6.48 | 126.12 | 3178.29 | 84.6% | 94.1% | 15.4% | 5.9% |
| | 5b | 6.24 | 6.39 | 613.24 | 1418.46 | 81.6% | 92.5% | 18.4% | 7.5% |
| | 6a | 6.91 | 9.06 | 110.68 | 267.70 | 78.5% | 88.4% | 21.5% | 11.6% |
| | average | 7.23 \pm 0.52 | 7.12 \pm 0.74 | 591.8 \pm 1160.6 | 3253.1 \pm 5204.6 | 84.5% \pm 5.7% | 92.4% \pm 2.3% | 15.5% \pm 5.7% | 7.6% \pm 2.3% |
| Ga'ïdat samples | 7a | 6.91 | 7.10 | 70.01 | 205.79 | 82.8% | 95.1% | 17.2% | 4.9% |
| | 7b | 7.25 | 6.90 | 98.16 | 955.86 | 87.7% | 93.2% | 12.3% | 6.8% |
| | 8a | 6.91 | 7.17 | 1077.74 | 346.78 | 73.9% | 90.2% | 26.1% | 9.8% |
| | 9a | 7.46 | 7.12 | 75.53 | 534.32 | 77.5% | 89.4% | 22.5% | 10.6% |
| | 10a | 7.45 | 7.33 | 59.55 | 199.91 | 74.2% | 90.1% | 25.8% | 9.9% |
| | 11a | 7.63 | 6.84 | 418.21 | 3330.37 | 84.4% | 91.9% | 15.6% | 8.1% |
| | 11b | 7.11 | 7.11 | 68.08 | 97.41 | 83.6% | 85.3% | 16.4% | 14.7% |
| | 12a | 6.44 | 6.34 | 540.50 | 2783.86 | 81.7% | 89.2% | 18.3% | 10.8% |
| | 12b | 7.72 | 6.87 | 508.47 | 3442.72 | 87.0% | 92.2% | 13.0% | 7.8% |
| | | average | 7.21 \pm 0.41 | 6.97 \pm 0.29 | 324.0 \pm 348.3 | 1321.9 \pm 1430.8 | 81.4% \pm 4.8% | 90.7% \pm 2.8% | 18.6% \pm 5.1% |

581

582

1
2
3
4
5
6
7 **583 Figure Legends**

8
9 584 Figure 1: Sampling locations in the Tindouf Basin region in southeastern
10
11 585 Morocco.

12
13 586 Figure 2: Image showing the two locations where pits were dug, the first at a
14
15 587 location in which the soil was covered with desert pavement (foreground) and a
16
17 588 second one nearby without substantial pavement (upper left corner).

18
19
20 589 Figure 3: The interquartile range (IQR), normalized against the total measured
21
22 590 anionic content, for the distribution of (a) Nitrate, (b) Sulfate, and (c) Chloride

23
24 591 Figure 4: Logarithmic plot showing the linear correlation (line) of the
25
26 592 concentrations of sulfate (blue), nitrate (red), and perchlorate (green), with the
27
28 593 concentration of chloride for the Moroccan soil samples from this study.

29
30 594 Figure 5: Logarithmic plots of oxyanion vs chloride concentrations for sulfate
31
32 595 (blue), nitrate (red), and perchlorate (green), for samples from Morocco (linear fit
33
34 596 lines from Fig. 3) compared to samples, from (a) Atacama (b) Beacon Valley (c)
35
36 597 University Valley (d) Taylor Valley (e) Victoria Valley (f) Mars, (symbols).

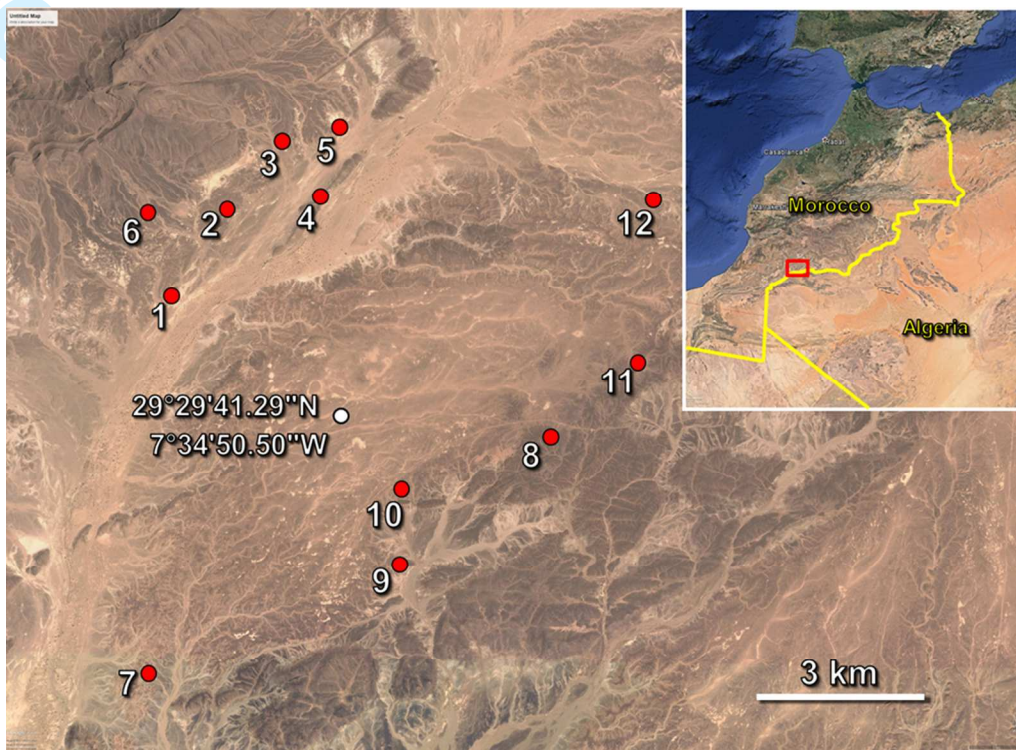
37
38 598 Figure 6: Correlation of nitrate and perchlorate concentrations for all the Mars
39
40 599 analog sites in this study.

41
42
43 600 Figure 7: Correlation of NO_3/ClO_4 and Cl/NO_3 average ratios for each martian
44
45 601 analog site.

46
47
48 602 Figure 8: Proposed martian epochs most relevant to “Mars analog sites”, based
49
50 603 on soil anion geochemistry and aridity .

51
52 604

605 **Figure 1**



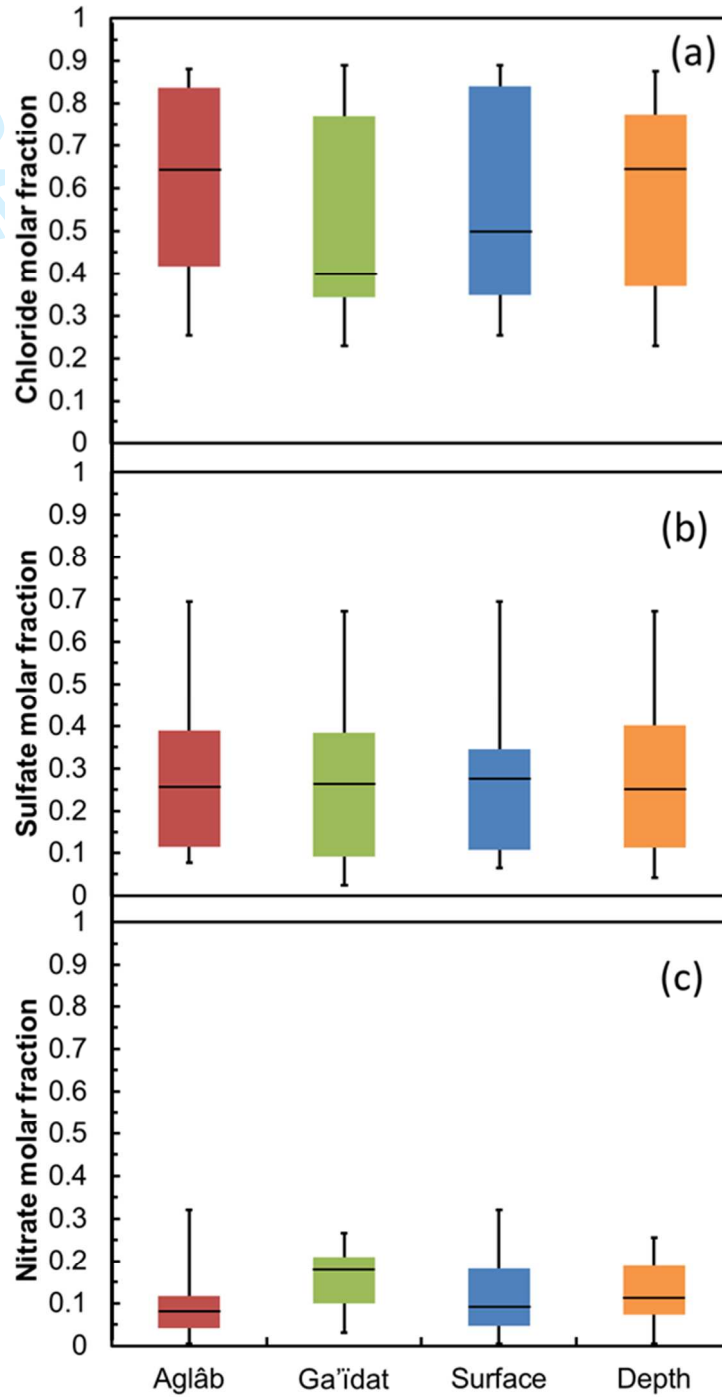
606

607 **Figure 2**



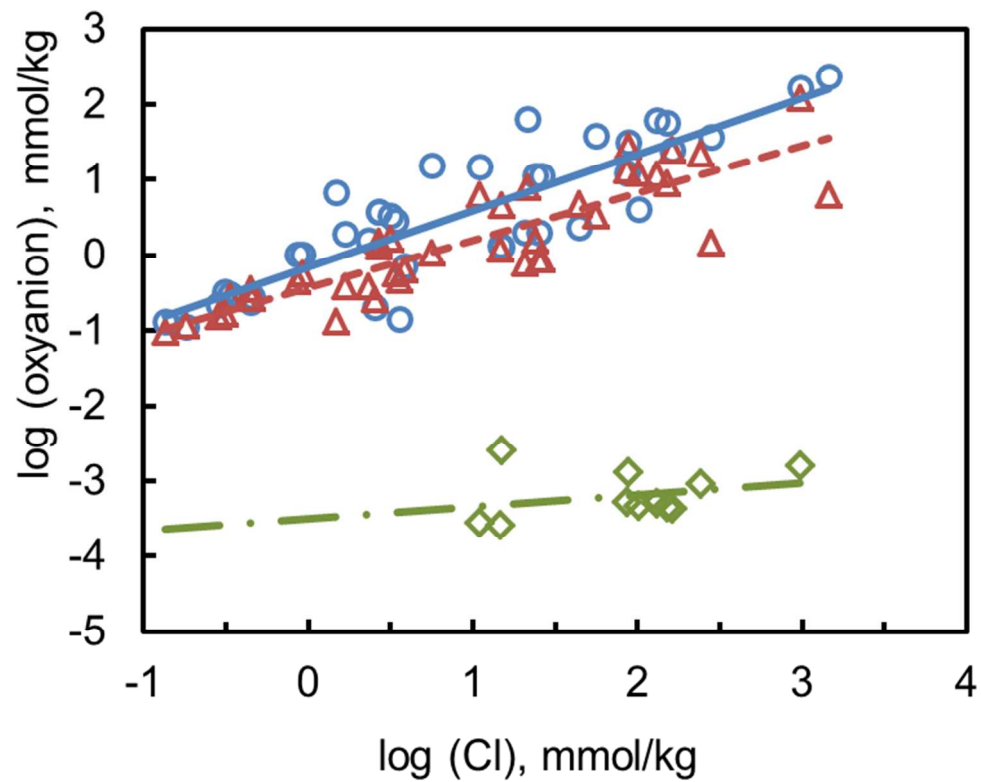
608

609 **Figure 3**



610

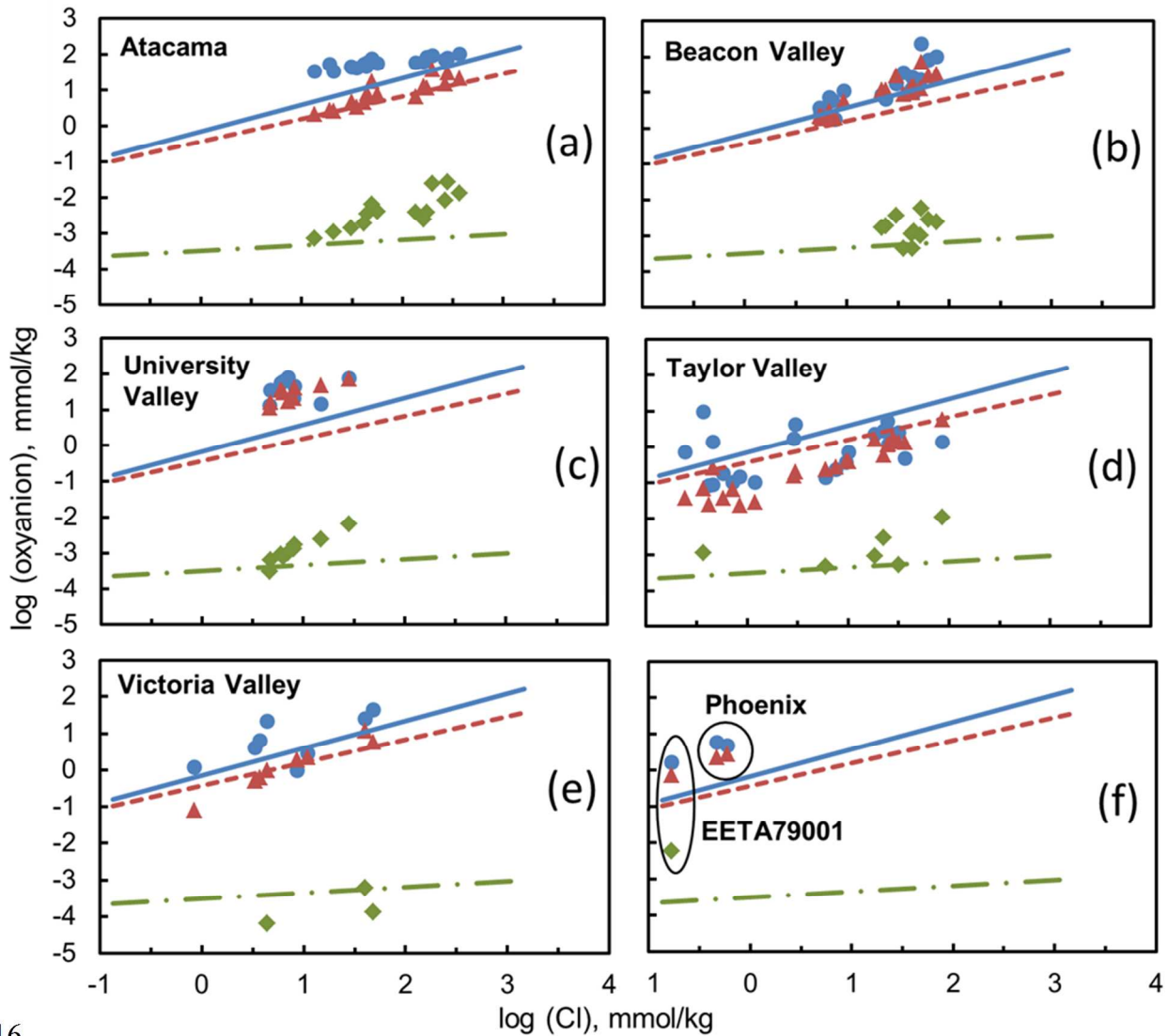
611

Submitted to *Astrobiology (Special Issue)*612 **Figure 4**

613

614

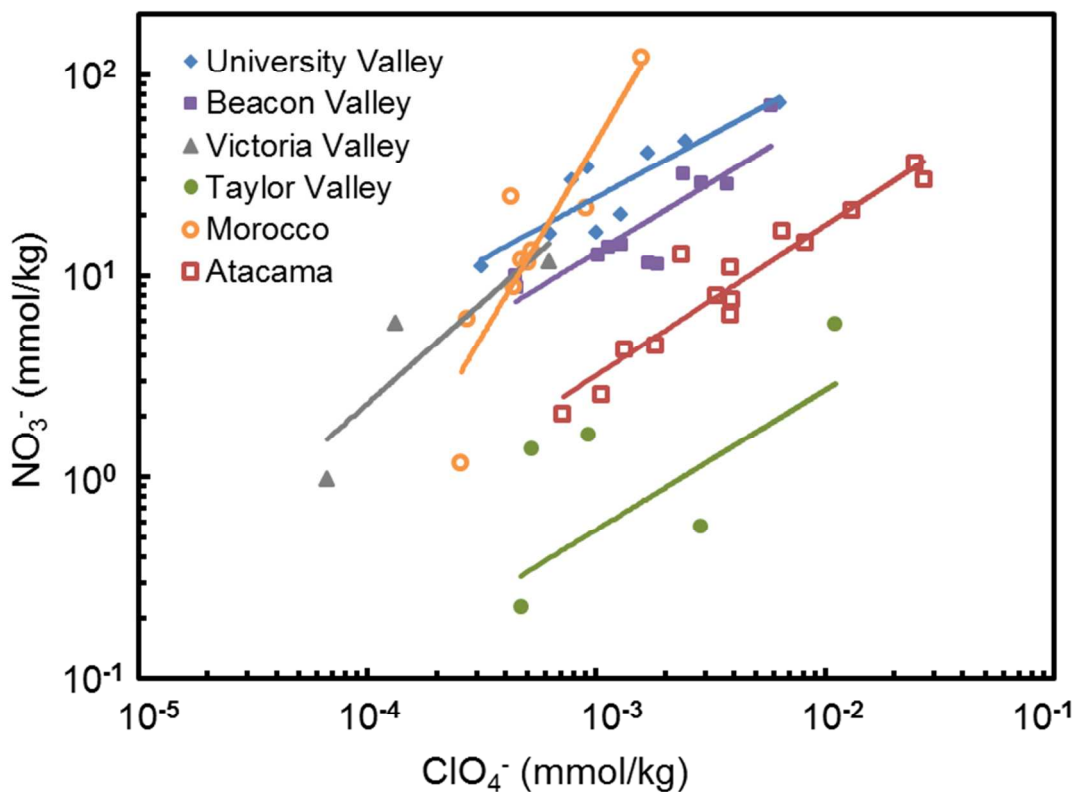
615 **Figure 5**



616
617

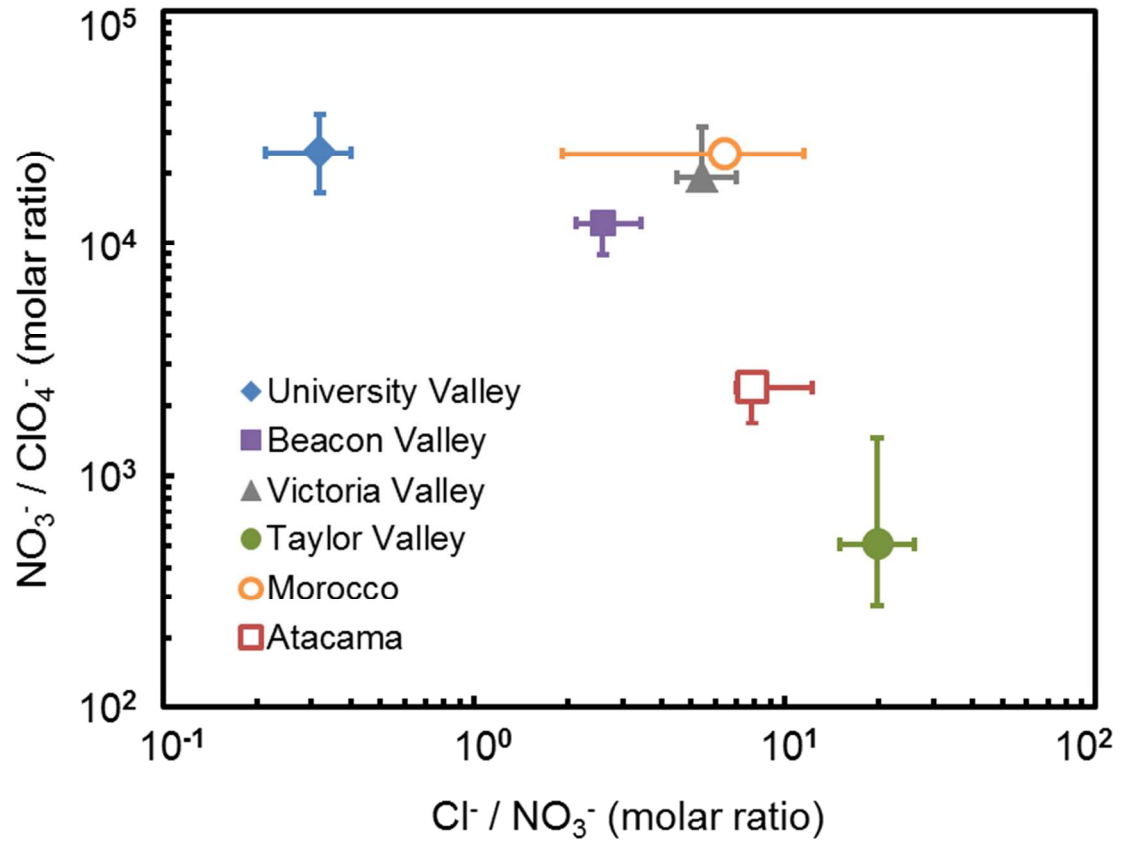
Distribution

618 **Figure 6**



619
620

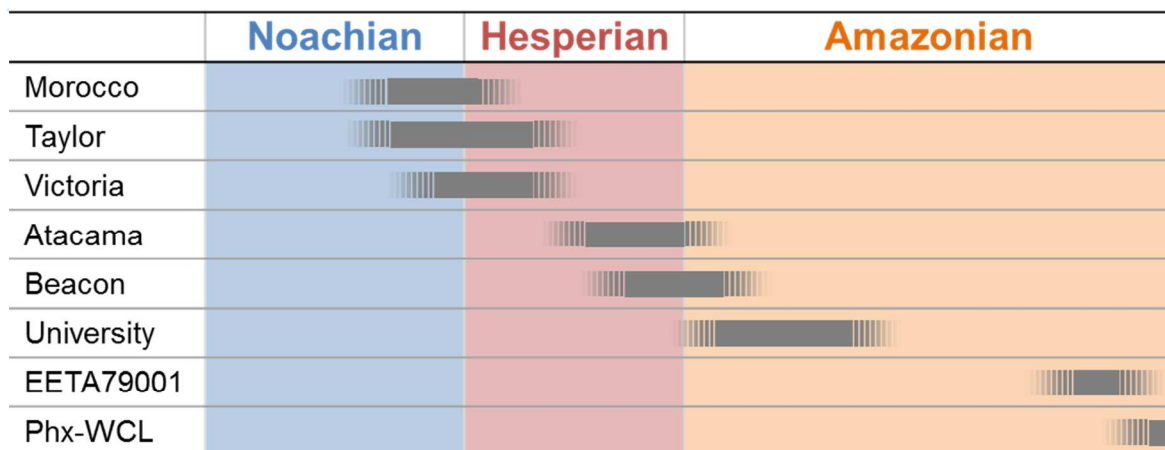
621 **Figure 7**



622
623

Submitted to *Astrobiology (Special Issue)*

624
625 **Figure 8**



626
627